Standing wave total internal reflection fluorescence microscopy to measure the size of nanostructures in living cells

Olga Gliko
Baylor College of Medicine
Department of Otolaryngology—Head & Neck Surgery
One Baylor Plaza, NA516
Houston, Texas 77030

Gaddum D. Reddy
Bahman Anvari
Rice University
Department of Bioengineering
Houston, Texas 77005

William E. Brownell
Baylor College of Medicine
Department of Otolaryngology—Head & Neck Surgery
One Baylor Plaza, NA516
Houston, Texas 77030

Peter Saggau
Baylor College of Medicine
Department of Neuroscience
One Baylor Plaza, S603
Houston, Texas 77030

Abstract. We present the first application of standing wave fluorescence microscopy (SWFM) to determine the size of biological nanostructures in living cells. The improved lateral resolution of less than 100 nm enables superior quantification of the size of subcellular structures. We demonstrate the ability of SWFM by measuring the diameter of biological nanotubes (membrane tethers formed between cells). The combination of SWFM with total internal reflection (TIR), referred to as SW-TIRFM, allows additional improvement of axial resolution by selective excitation of fluorescence in a layer of about 100 nm.
[DOI: 10.1117/1.2372457]

Keywords: resolution; fluorescence; interference; phase shifts; image reconstruction; point spread functions.

Paper 06097LRR received Apr. 10, 2006; revised manuscript received Aug. 29, 2006; accepted for publication Aug. 31, 2006; published online Nov. 14, 2006.

1 Introduction

The importance of real-time observations of dynamic processes in living cells inspires the development of noninvasive high-resolution imaging techniques. Fluorescence-based far-field microscopy is the most employed technique for quantitative three-dimensional (3D) molecular specific imaging of live biological specimens. The spatial resolution of far-field microscopy is limited by the smallest possible size of a light spot produced by the focusing optics. The size of this light spot is defined by the point-spread function (PSF), and resolution can be quantified as the full width at half maximum (FWHM) of the PSF. For fluorescence with a peak emission wavelength of λ_{em}=520 nm, collected by an objective lens with a numerical aperture (NA) of 1.45, the calculated lateral resolution in the imaging plane is Δx, $\Delta y \sim \lambda_{em}/2\mathrm{NA}$ $\sim$180 nm. The axial resolution is $\sim$3 to 4 times lower than the lateral resolution, compromising the 3D resolution and degrading the contrast in the imaging plane. Due to the strong optical scattering of biological specimens, this resolution limit is commonly not achieved.

There have been several approaches to improve resolution. The largest improvement of axial resolution, to a value of $\sim$100 nm, has been achieved by 4π microscopy.[1] Another technique, stimulated emission depletion microscopy, has thus far provided the best lateral resolution of $\sim$16 nm among far-field techniques.[2] However, both techniques are based on point scanning, which complicates their application to the study of fast processes. Another drawback is the low effective signal-to-noise ratio, which is critical for biological specimens with notoriously low fluorescence intensity.

One wide-field technique, standing wave fluorescence microscopy (SWFM), has been shown to improve lateral resolution to 100 nm, a factor greater than 2 compared with standard fluorescence microscopy. The resolution improvement is based on a periodic excitation pattern with high spatial frequency. The resolution of SWFM is determined by the FWHM of the effective PSF, which is equal to half of the period of the excitation pattern.[3] The axial resolution can be improved by total internal reflection fluorescence microscopy (TIRFM), which produces a thin excitation field at an interface where the refractive index steps down.[4] This evanescent field decays exponentially in the axial direction and is therefore ideal for selective excitation of fluorophores near a glass/water interface. TIRFM has the significant advantage of imaging with low background fluorescence. It allows single molecule visualization in real time.[5] Further improvement of

Address all correspondence to Peter Saggau, Department of Neuroscience, Baylor College of Medicine, One Baylor Plaza – S603, Houston, TX 77030; Tel: 713-798-5082; Fax: 713–798–3946; E-mail: psaggau@bcm.edu

1083-3668/2006/11(6)/064013/5/$22.00 © 2006 SPIE

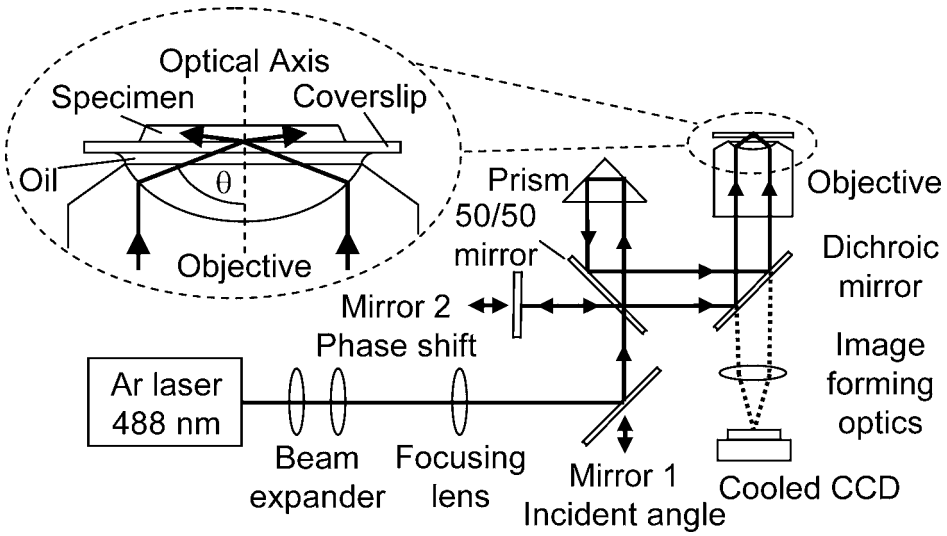

Fig. 1 Schematic of the standing wave total internal reflection fluorescence microscopy (SW-TIRFM) setup. The inset shows the interfering beams.

SWFM resolution can be achieved by using evanescent illumination.[6] The first experimental implementation was demonstrated with a standing wave evanescent field coupled through an objective lens.[7]

We have combined SWFM and TIRFM to achieve 3D resolution improvement by using the evanescent standing wave pattern to selectively excite the sample near a glass coverslip. Our technique allows real-time data acquisition for morphometric investigations of living cells with conventional wide-field detection. The standing wave was created at the focal plane of the objective lens of a standard inverted microscope. Our implementation allows switching between SWFM and combined SW-TIRFM, permitting the imaging of objects far from the coverslip or in close vicinity to it. Tests with fluorescent beads showed an effective PSF with a FWHM of <100 nm. We demonstrated the ability of this technique to measure the dimensions of nanometer-size living objects, membrane nanotubes.

2 Standing Wave Total Internal Reflection Fluorescence Microscopy

The experimental setup is shown in Fig. 1. Laser light (488 nm) was coupled into an objective lens of a standard inverted microscope. The use of the inverted microscope scheme simplified both the optical system and the experimental procedure. A specimen was placed in a standard Petri dish with a glass coverslip bottom, which allowed convenient electrophysiological recording and media replacement. We created a standing wave pattern by using a Michelson interferometer scheme. The optical layout of this interferometer was such that it resulted in two parallel beams with controllable separation (mirror 1) and phase delay (mirror 2). The beams were reflected by a dichroic mirror, and focused by a lens at the back focal plane of an oil immersion 100× objective lens with a high NA of 1.45. This procedure resulted in two collimated beams polarized normal to the incident plane. These beams interfered at the focal plane, creating a lateral periodic excitation pattern with closely spaced fringes.

The resulting intensity pattern in specimen plane can be described as $I(x)=1+\cos(Kx+\phi)$, where $K=4\pi n_{glass}\sin\theta/\lambda_{ex}$ is the spatial frequency of the standing wave, λ_{ex} is the excitation wavelength, $n_{glass}=1.52$ is the refractive index of glass, θ is the beam incident angle, and ϕ is the phase of interference pattern. The period of the resultant interference pattern is given as $\Delta s=\lambda_{ex}/(2n_{glass}\sin\theta)$. Moving mirror 1, placed after the focusing lens, allowed for variation of the spatial separation between the two beams and consequent adjustment of their incident angle at the focal plane. As a result, we were able to control the period of the standing wave pattern and also switch to TIR at incident angles above the critical angle of $\theta_c=61.2$ deg. Achieving TIR through an objective is only possible with a NA higher than the refractive index of water, $n_{water}\sim 1.3$. At the TIR condition, the standing wave pattern penetrates from the coverslip with its intensity decaying exponentially in the direction normal to the interface. The penetration depth decreases with increasing incident angle. Using a 1.45 NA objective lens, the largest angle of $\theta=72.8$ deg resulted in a minimal fringe spacing of $\Delta s=168$ nm and the smallest penetration depth of 67 nm ($1/e$ criterion).

The modulated excitation pattern caused fluorescent emission, which was intensity modulated with the same period as the excitation field. The fluorescence emitted by the specimen was collected by the same objective lens and passed through the dichroic mirror and an additional long-pass filter to block residual excitation light. The fluorescence image was then magnified and captured with a cooled charge-coupled device (CCD) camera. The phase of the standing wave pattern was precisely controlled by moving the piezoactuated mirror 2. A computer controlled movement of mirror 2 synchronized the image acquisition sequence of the camera. Data collection involved acquiring an image for each of three different phases ϕ, $\phi+\pi/2$, $\phi+\pi$ of the excitation pattern (i.e., at three different fringe positions relative to the specimen). The SWFM reconstructed image was calculated as the sum of the three acquired images weighted by sinusoidal factors that depend

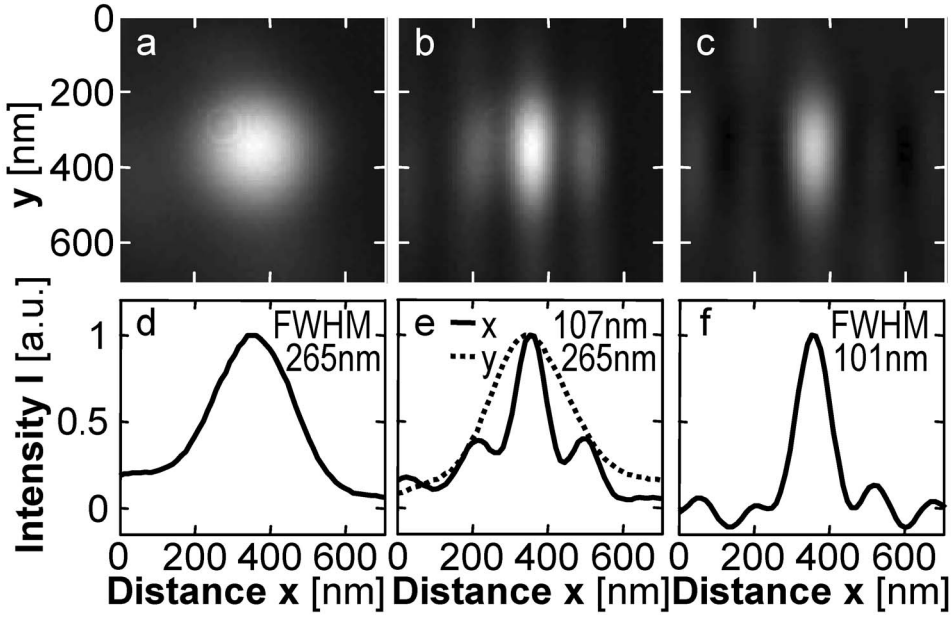

Fig. 2 Imaging subresolution fluorescent beads using SW-TIRFM. (a) TIRFM, (b) SW-TIRFM reconstructed, and (c) deconvolved SW-TIRFM images, (d) intensity profile along the *x* direction of (a) indicates resolution of standard microscopy, (e) intensity profiles of (b) along the *x* and *y* directions through bead center shows an improved resolution in the *x* direction, (f) intensity profile of (c) shows removed side lobes and narrowed central peak compared to SW-TIRFM *x* profile.

on the period and phase of the standing wave.[6,8] The resulting reconstructed SWFM image had an enhanced lateral resolution equal to half the fringe spacing in the direction normal to the interference fringes. The maximum achievable resolution with and without TIR was 84 nm and 92 nm, respectively.

3 SW-TIRFM Resolution Test

We tested the stability of the standing wave phase by imaging the excitation pattern with the emission filter removed. Due to the compact design of the interferometer, thermal drift was insignificant for periods shorter than 1 min. The sensitivity of the cooled CCD camera allowed exposure time to be as short as 1 s.

To test the resolution of our SW-TIRFM system, we imaged fluorescent beads with a known diameter of 100 nm, which is below the resolution limit of standard microscopy. A portion of the beads suspended in water would adhere to a polylysine coated coverslip. Utilizing TIR improved the axial resolution, which resulted in high contrast images, with very bright beads adjacent to glass and a dark background undisturbed by nonadhered beads. Both TIRFM and reconstructed SW-TIRFM images of a 100-nm bead are shown in Figs. 2(a) and 2(b), respectively. The intensity profiles taken in two perpendicular directions, normal and parallel to the fringes of the reconstructed SWFM image [Fig. 2(e)] showed that the FWHM was 107 nm and 265 nm, respectively. The FWHM of the intensity profile taken of the TIRFM image was 265 nm [Fig. 2(d)]. This demonstrates a one-dimensional lateral resolution improvement, as measured by the FWHM, by a factor of greater than two compared with standard widefield microscopy. The resolution is enhanced in the direction normal to interference fringes. The intensity profile has two side lobes, which are intrinsic features of SWFM resulting from the convolution of an object with the effective PSF of SWFM, which is in turn a product of standard PSF and excitation standing wave intensity. Since the side lobes were below 50% of central maximum, the object size can be unambiguously extracted by linear deconvolution. We used a method known as inverse filtering:[8] the Fourier transform of the reconstructed SWFM image was divided by the effective optical transfer function (OTF) of SWFM, then transformed back using only values within the bandwidth of the effective OTF. To obtain the effective PSF, we multiplied the intensity profile of the TIRFM image of a 100-nm bead by the measured standing wave pattern. The result of linear deconvolution applied to SWFM image [Fig. 2(b)] is shown in Fig. 2(c). The corresponding intensity profile [Fig. 2(f)] indicates removed side lobes and a narrowed central peak compared to the *x* profile in Fig. 2(e). The object size can be determined from the FWHM of the intensity profile of deconvolved image. The average diameter of six beads was 101 ± 6 nm. Therefore, our method allows to determine object sizes of at least 100 nm with an accuracy of 6 nm.

4 SWFM Application to Live Cells

The performance of SWFM with biological samples was evaluated by imaging biological nanotubes, that is, membrane tethers, between living cells. The formation of cell membrane tethers is a general phenomenon occurring during cell adhesion, communication, and spreading.[9] Membrane tethers can also be pulled from a cellular plasma membrane using a microsphere attached to the membrane and manipulated by optical tweezers.[10] These experiments give insight into the physics of tether formation as well as the mechanics of cell membranes. Optical tweezers in combination with patch-clamp techniques allow the investigation of electromechanical

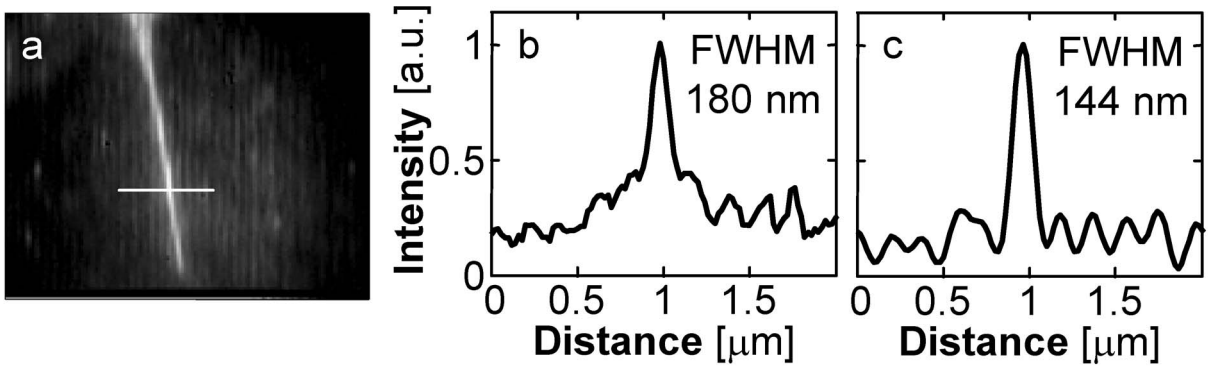

Fig. 3 Imaging membrane tether formed between HEK cells. (a) SWFM reconstructed image, (b) intensity profiles taken across the tether along the line depicted in (a), (c) was obtained from (b) by applying linear deconvolution. The tether diameter was determined as 144 nm, based on FWHM of the deconvolved SWFM image profile.

properties of plasma membranes by measuring the mechanical response of membrane tethers to changes in the transmembrane potential.[11] Direct measurement of the tether diameter is necessary for the analysis of voltage-induced force generation. So far it has not been possible to measure tether diameter by light microscopy, because the tether is considerably thinner than the lateral resolution of conventional light microscopy. Scanning electron microscopy (SEM) performed on fixed cells has shown that tethers are 50 to 200-nm thick.[9]

We applied our SWFM setup to determine the diameter of membrane tethers formed spontaneously between cultured human embryonic kidney (HEK) cells. These tethers stretch between interconnected cells and are up to several cell diameters in length.[9] Because most of the tethers do not contact the substrate, we did not utilize TIR in this case. The cell membrane was stained with a fluorescent label Alexa Fluor 488 conjugated to wheat germ agglutinin, a lectin that binds with the membrane. The cells were cultured in a Petri dish. The label was added directly to the culture medium (50-μg/ml final concentration) and washed away after a 15-min incubation. The Petri dish with cells was placed onto the translational stage of the microscope. The diameter of the tethers oriented about parallel to the standing wave fringes was determined by the FWHM of the intensity profile of the deconvolved SWFM image. A SWFM image of the tether, the corresponding intensity profile taken along the depicted horizontal line, and deconvolved intensity profile are shown in Figs. 3(a)–3(c), respectively. Diameters of tethers as determined by FWHM measurements were in the range from 140 to 270 nm. These values agree with those obtained from SEM measurements.[9] To our knowledge, this is the first measurement of the diameter of a membrane tether from a living cell.

5 Conclusions

We have developed a technique to study biological nanostructures in living cells. SW-TIRFM through an objective lens improved lateral and axial resolutions. Data collection and analysis are easy and rapid, and free access to the specimen during the experiment is retained. In addition, there is no limit to the thickness of specimen. An effective PSF with side lobes below 50% allows size determination with $<$100-nm resolution from the intensity profile of the linearly deconvolved SWFM image. In addition, if the object size is in the range of 20 to 180 nm, it can be extracted from the ratio between the average value of the two side minima and the central maximum.[12] Using this technique, we determined the diameter of spontaneously formed membrane tethers. This is the first application of SWFM to measure the nanometer-sized structure in live biological specimens. This technique can provide real-time size measurements as the total acquisition time does not exceed 1 s. Improved two-dimensional resolution can be achieved by rotating the standing wave pattern relative to the specimen and acquiring additional images. By changing the incident angle, it is possible to switch between SWFM and SW-TIRFM. SWFM allows 3D imaging by acquiring a series of images while changing the focal plane through the specimen. SW-TIRFM provides an additional improvement of axial resolution and contrast by exciting a thin section of the specimen adjacent to coverslip. With the appropriate choice of fluorescent labels, this optical setup can be used to image both the interior and surface of cells. Therefore, potential applications include studying processes occurring near the cell membrane, such as exocytosis and endocytosis, as well as cell adhesion, spreading and communication. Imaging accompanied by electrophysiological measurements should make it possible to relate structural changes to physiological cell-signaling events. Structural transformations inside the cell, such as those occurring in the Golgi apparatus and DNA complexes, can be studied as well.

Further resolution improvement of SW-TIRFM could be achieved by utilizing nonlinear excitation.[13] Then resolution is only limited by the signal-to-noise ratio, which in turn is limited by photobleaching. Using highly photostable fluorophores, such as quantum dots, makes this approach potentially applicable to living samples. It has also been suggested that 3D resolution is achievable by using a standing wave pattern formed in selected orientations in space.[14]

Acknowledgments

We thank Abbas Yaseen, Brad Losavio, and Mark Pierce for experimental support and suggestions. This work was supported by grants from the National Institute of Health and National Science Foundation to B.A., W.E.B., and P.S.

References

1. A. Egner, S. Jakobs, and S. W. Hell, "Fast 100-nm resolution three-dimensional microscope reveals structural plasticity of mitochondria in live yeast," *Proc. Natl. Acad. Sci. U.S.A.* **99**(6), 3370–3375 (2002).
2. V. Westphal and S. W. Hell, "Nanoscale resolution in the focal plane of an optical microscope," *Phys. Rev. Lett.* **94**(14), 143903 (2005).
3. J. T. Frohn, H. F. Knapp, and A. Stemmer, "True optical resolution beyond the Rayleigh limit achieved by standing wave illumination," *Proc. Natl. Acad. Sci. U.S.A.* **97**(13), 7232–7236 (2000).
4. D. Axelrod, "Cell-substrate contacts illuminated by total internal reflection fluorescence," *J. Cell Biol.* **89**(1), 141–145 (1981).
5. A. Sonnleitner, L. M. Mannuzzu, S. Terakawa, and E. Y. Isacoff, "Structural rearrangements in single ion channels detected optically in living cells," *Proc. Natl. Acad. Sci. U.S.A.* **99**(20), 12759–12764 (2002).
6. G. E. Cragg and P. T. C. So, "Lateral resolution enhancement with standing evanescent waves," *Opt. Lett.* **25**(1), 46–48 (2000).
7. E. Chung, D. Kim, and P. T. C. So, "Extended resolution wide-field optical imaging: Objective-launched standing-wave total internal reflection fluorescence microscopy," *Opt. Lett.* **31**(7), 945–947 (2006).
8. V. Krishnamurthi, B. Bailey, and F. Lanni, "Image processing in 3-D standing-wave fluorescence microscopy," *Proc. SPIE* **2655**, 18–25 (1996).
9. A. Rustom, R. Saffrich, I. Markovic, P. Walther, and H.-H. Gerdes, "Nanotubular highways for intercellular organelle transport," *Science* **303**, 1007–1010 (2004).
10. J. Dai and M. P. Sheetz, "Mechanical properties of neuronal growth cone membranes studied by tether formation with laser optical tweezers," *Biophys. J.* **68**(3), 988–996 (1995).
11. F. Qian, S. Ermilov, D. Murdock, W. E. Brownell, and B. Anvari, "Combining optical tweezers and patch clamp for studies of cell membrane electromechanics," *Rev. Sci. Instrum.* **75**(9), 2937–2942 (2004).
12. A. V. Failla, U. Spoeri, B. Albrecht, A. Kroll, and C. Cremer, "Nanosizing of fluorescent objects by spatially modulated illumination microscopy," *Appl. Opt.* **41**(34), 7275–7283 (2002).
13. M. G. Gustafsson, "Nonlinear structured-illumination microscopy: Wide-field fluorescence imaging with theoretically unlimited resolution," *Proc. Natl. Acad. Sci. U.S.A.* **102**(37), 13081–13086 (2005).
14. J. T. Frohn, H. F. Knapp, and A. Stemmer, "Three-dimensional resolution enhancement in fluorescence microscopy by harmonic excitation," *Opt. Lett.* **26**(11), 828–830 (2001).